HHS Public Access

Author manuscript

IEEE J Sel Top Quantum Electron. Author manuscript; available in PMC 2020 January 01.

Published in final edited form as:

IEEE J Sel Top Quantum Electron. 2019 ; 25(1): . doi:10.1109/JSTQE.2018.2833455.

Viscosity monitoring during hemodiluted blood coagulation using optical coherence elastography

Xiangqun Xu[*],

College of Life Sciences, Zhejiang Sci-Tech University, Hangzhou, Zhejiang 310018, China, and the Beckman Laser Institute, University of California, Irvine, Irvine, California 92612, USA

Jiang Zhu[*]

Beckman Laser Institute, University of California, Irvine, Irvine, California 92612, USA

Junxiao Yu, **Zhongping Chen**

Department of Biomedical Engineering, and the Beckman Laser Institute, University of California, Irvine, Irvine, California 92612, USA

Abstract

Rapid and accurate clot diagnostic systems are needed for the assessment of hemodiluted blood coagulation. We develop a real-time optical coherence elastography (OCE) system, which measures the attenuation coefficient of a compressional wave induced by a piezoelectric transducer (PZT) in a drop of blood using optical coherence tomography (OCT), for the determination of viscous properties during the dynamic whole blood coagulation process. Changes in the viscous properties increase the attenuation coefficient of the sample. Consequently, dynamic blood coagulation status can be monitored by relating changes of the attenuation coefficient to clinically relevant coagulation metrics, including the initial coagulation time and the clot formation rate. This system was used to characterize the influence of activator kaolin and the influence of hemodilution with either NaCl 0.9% or hydroxyethyl starch (HES) 6% on blood coagulation. The results show that PZT-OCE is sensitive to coagulation abnormalities and is able to characterize blood coagulation status based on viscosity-related attenuation coefficient measurements. PZT-OCE can be used for point-of-care testing for diagnosis of coagulation disorders and monitoring of therapies.

Keywords

Biomedical optical imaging; biomechanics; optical coherence elastography; blood coagulation; viscosity; optical coherence tomography

I. Introduction

Perioperative bleeding in trauma and surgery is often referred to as coagulopathic bleeding. Changes in the blood coagulation system in the perioperative period include

xuxiangqun@zstu.edu.cn.

[*]First two authors contributed equally to this work

X. Xu and J. Zhu contributed equally to this work and are treated as co-first authors.

hyperfibrinolysis and coagulopathy due to blood loss, consumption, dilution, hypothermia, acidosis, hypocalcemia and anticoagulation. These coagulopathic changes in massive bleeding may result in a defect in clot firmness due to fibrinogen deficiency (an early phenomenon) and thrombocytopenia, impair clot stability due to hyperfibrinolysis and factor XIII deficiency (a late phenomenon), and prolong clot generation due to various coagulation factor deficiencies [1]. Infusion therapy is essential in intravascular hypovolemia and extravascular fluid deficits. Severe bleeding requires intensive intravenous fluid infusion, and crystalloids and colloids as plasma expanders are commonly used. Hydroxyethyl starch (HES) is a colloid solution that can be used to replace initial blood loss and to treat hypovolemia during surgeries. The local routine at hospitals is to use HES 130/0.42 (molecular weight 130 kD and substitution degree of 0.42) for hemodynamic stabilization and initial blood loss replacement [1, 2]. However, crystalloids and colloids have significant anticoagulant side-effects and could cause dilutional coagulopathy. Monitoring early signs of side-effects could avoid the risk [1]. Therefore, prompt monitoring of blood coagulation is essential for the management of hypofibrinogenemia due to hemodilution.

Routine coagulation analysis includes the measurement of activated partial thromboplastin time (aPTT), prothrombin time (PT), platelet count and fibrinogen levels in plasma, which usually take 30 to 60 minutes. Thromboelastography and thromboelastometry (TEG/ROTEM), viscoelasticity measurements for point-of-care testing, allow the assessment of clot formation process and fibrin polymerization in whole blood for diagnosing disorders and monitoring therapy [3]. Point-of-care testing allows individual patient management with specific, targeted, and rapid supplementation of depleted coagulation factors [4, 5]. However, TEG/ROTEM are not ideal for assessing clot mechanical properties due to poor sensitivity and repeatability and lack of standardization [3, 6]. The poor standardization of TEG/ROTEM may be partly due to the absence of standard clinical protocols and accurate measurements of the stress and strain.

Recently, optical coherence elastography (OCE), employing optical coherence tomography (OCT) to detect sample deformation, sample vibration or shear wave propagation, has been developed to assess tissue biomechanics [7, 8]. OCT techniques offer distinct features, including spatial resolution of ~10 μm, acquisition speed above 50 kHz, and three-dimensional, unlabeled and noninvasive imaging [9–11]. Excitation approaches and elastic determination are generally two characteristics of an OCE system. Various excitation approaches have been proposed to induce vibrations in the samples, such as the use of a piezoelectric (PZT) actuator for contact stimulation [12], the use of an air-puff device for noncontact stimulation [13], and the application of acoustic radiation force (ARF) for remote excitation [14–16]. PZT excitation is convenient for applying force onto the sample and inducing vibrations. For elastic determination, local strain [17], shear wave velocity [15, 18], vibration amplitude [19–21] and resonance frequency [22] have been developed to assess mechanical properties. OCE based on vibration measurements has the advantage of enabling real-time assessment without complex data capture and analysis. Therefore, the PZT-OCE device can conveniently and sensitively monitor the changes of viscoelastic properties in real-time.

In this study, we report on the development of a PZT-OCE system that enables real-time monitoring of viscosity in a single drop of blood during the dynamic blood coagulation process. Porcine blood was tested as the model because the properties of porcine blood are similar to human blood, particularly in the coagulation process. The tests with porcine blood can be regarded as a safe estimation for human blood. First, we validated the feasibility of PZT-OCE for characterization of viscous properties of blood samples. Then we monitored the tracings of viscosity-related attenuation coefficients during blood coagulation and developed coagulation metrics to assess blood coagulation properties. We compared the changes of coagulation metrics between the samples with different concentrations of activator kaolin solutions to validate this method. Finally, we detected the blood coagulation process among the samples with different hemodilution which is commonly used in infusion therapy.

II. Materials and Methods

A. System setup

The properties of blood coagulation were monitored based on the measurements of viscosity-related attenuation coefficients of blood samples using PZT-OCE. The PZT-OCE system is shown in Fig. 1. The PZT was driven by 1 cycle of sine wave with a frequency of 200 Hz and a peak-to-peak voltage of 70.8 v. After a drop of porcine blood with a volume of 200 μL was injected onto the microscope slide, the PZT was moved downwards to touch the top surface of the blood drop, and then the PZT was moved upwards. The distance between the lower surface of the PZT and the upper surface of the microscope slide was 2 mm. Due to the surface tension of the blood drop, the sample was attached between the PZT and microscope slide, and the thickness of the blood drop was 2 mm through the whole measurements. At the beginning of the measurements, the blood drop was attached between the PZT and microscope slide due to the surface tension. During the blood coagulation, the blood drop was attached firmly with the PZT and the slide due to the adhesive force. So the thickness of the blood sample was not changed during the measurements. The contact area between the PZT and the blood drop was ~64 mm^2 (diameter of ~9.0 mm) and the contact area between microscope slide and the blood drop was ~141 mm^2 (diameter of ~13.4 mm). As the thickness of the blood drop was only 2 mm, the flat structure of the blood drop was relatively stable due to the surface tension and adhesive force during the measurements.

The OCT scan lens was located on the opposite side of the blood sample, and the OCT beam passed through the microscope slide. The vibrations in the blood drop were detected by the OCT system based on a swept source with a central wavelength of 1310 nm and an A-line speed of 50 kHz. The light from the laser source was split into the sample arm and the reference arm with a power of 90% and 10%, respectively. For vibration detection, 1000 A-lines, corresponding to a total time of 20.0 ms, were recorded in one OCT M-scan during which the PZT amplifier started to drive the PZT at 2.0 ms. The PZT-induced vibration was parallel to the OCT beam and was detected by Doppler phase shift measurements. The Doppler phase shift $\Delta\varphi$ measured by the OCT system was used to calculate the vibration velocity V by the following equation:

$$V = \frac{\lambda_0 \times \Delta\psi}{4\pi \times n \times \Delta t} \quad (1)$$

where λ_0 is the vacuum center wavelength, n is the refractive index, and Δt is the time interval. The parameters of λ_0 and n were 1310 nm and1.4 [10, 23–25]. Due to the limitation of the OCT signal-to-noise ratio, $\Delta\psi$ cannot be accurately measured when V is too low. The increase of Δt will increase the phase change $\Delta\psi$ for the same velocity and, thus, improve the accuracy of the velocity measurement [10]. However, if the A-line interval Δt is too large, the phase wrap will occur and the unwrapping correction is required. The optimized time interval Δt is 0.10 ms for measurement in the blood sample and is 0.02 ms for measurement on the PZT surface.

B. Sample preparation for feasibility test

The feasibility of PZT-OCE was investigated in the clotting blood. Fresh citrated porcine whole blood (Sierra for Medical Science, CA) of 600 μL was recalcified with buffered $CaCl_2$ (0.2 mol/L, 40 μL) and gently mixed with the activator kaolin solution (12.8 g/L, 40 μL). The final concentrations of $CaCl_2$ and kaolin were 0.01 mol/L and 0.75 g/L, respectively. Then, 200 μL of the final reaction mixture was slowly injected onto the microscope slide and immediately measured by the PZT-OCE system.

C. Sample preparation for hemodilution test

In order to quantify the viscous changes during blood coagulation, the changes in the attenuation coefficient and coagulation metrics were measured, which included the initial coagulation time when the attenuation coefficient starts to become larger and the clot formation rate during the attenuation coefficient increases dramatically.

In the first experimental series, different concentrations of activator kaolin solutions (final concentrations of 0.75 g/L and 0.38 g/L) were added to the blood sample. In the feasibility test, three samples for each group were tested for 10 min, and the changes of coagulation metrics were measured. Then, we added kaolin solutions with a final concentration of 0.38 g/L and diluted samples of citrated porcine whole blood with either NaCl 0.9% (Sigma-Aldrich, MO) or VetStarch HES 6% 130/0.4 (Zoetis, NJ). Following the same procedure, derived coagulation metrics were measured by the PZT-OCE system.

III. Results and Discussion

A. Feasibility test

Time-course coagulation of the citrated porcine blood was monitored by measurements of the viscosity-related attenuation coefficient of a compressional wave propagating in the blood drop. After PZT vibration in a cycle of sine wave induced a compressional wave inside the blood drop, the compressional wave propagated from the top surface to the bottom surface of the blood drop. Due to attenuation of a compressional wave, the displacement amplitude of the compressional wave was decreased. Based on power-law frequency-dependent attenuation equation in viscoelastic media [26, 27]:

$$A(\Delta x) = A(0) \cdot e^{-\alpha \cdot \Delta x} \quad (2)$$

where A(0) and A(Δ*x*) are the amplitudes of a compressional wave at the initial position and after the wave travels a distance of Δ*x*, respectively, and α is the frequency-dependent attenuation coefficient. The attenuation coefficient α of a compressional wave is associated with the properties of tissue scattering and tissue absorption [28]. In our measurements, the wavelength of the compressional wave was ~7.5 m (with a wave frequency of 200 Hz and a wave velocity of ~1.5×10^3 m/s), which is much larger than the scatters of blood cells (several micrometers). Therefore, the attenuation due to tissue scattering can be ignored. The tissue absorption mechanisms include viscosity and thermal conduction. In comparison to the absorption due to viscous relative motion, the absorption due to thermal conduction is negligible [28]. Due to the low scattering contributions and thermal losses, the attenuation of the compressional wave measured in our study mainly depended on the tissue viscosity with a given wave frequency.

We quantified the attenuation coefficient to assess the tissue viscosity. The ratio of displacement amplitude $A(\Delta x)$ to $A(0)$ is equal to the ratio of maximum vibration velocity $V_{max}(\Delta x)$ at a distance of Δx to $V_{max}(0)$ at the initial position because the PZT is driven by a sine function in this study and the velocity is the time derivative of the displacement. Equation 2 can be transferred to the following equation:

$$\ln\left[\frac{A(\Delta x)}{A(0)}\right] = \ln\left[\frac{V_{max}(\Delta x)}{V_{max}(0)}\right] = -\alpha \cdot \Delta x \quad (3)$$

Thus, the attenuation coefficient α can be calculated by the following equation:

$$\alpha = \frac{\ln[V_{max}(0)] - \ln[V_{max}(\Delta x)]}{\Delta x} \quad (4)$$

After predetermination of the maximum PZT vibration velocity $V_{max}(0)$, the attenuation coefficient α can be calculated by measurements of the maximum vibration velocity $V_{max}(\Delta x)$ after the wave travels a distance of Δ*x*.

Figure 2A shows the OCT image in B-mode at 1 min after kaolin addition. M-scans were captured at the position indicated by the red arrow in Fig. 2A and were analyzed by the Doppler phase shift method. One M-scan OCT image captured at 1 min following the recalcification is shown in Fig. 2B, and the corresponding Doppler phase image is shown in Fig. 2C. From the Doppler phase image, vibration velocities at 1.4 mm away from the PZT surface were analyzed (i.e. the region in the dashed box in Fig. 2C), which is shown in Fig. 2D. We also measured the vibration velocities on the PZT surface by Doppler OCT without loading the blood drop, which is shown in Fig. 2D. The vibration velocities on the PZT surface and in the blood drop change over time during one cycle of the PZT excitation and reached a maximum at ~6.5 ms in Fig. 2D. The attenuation coefficient α is 1.1 Np/mm when Δx is 1.4 mm, the $V_{max}(0)$ and $V_{max}(1.4)$ are 4.0 mm/s and 0.9 mm/s, respectively. This measurement position in the blood drop is selected in order to get higher OCT signal-to-noise ratio and avoid the distortion due to the reflection of the compressional wave near the

surface of the microscope slide. The attenuation coefficient α depends on the viscous property of the blood with a given frequency of sine wave excitation, and is independent on the PZT loading placement.

B. Blood coagulation with different kaolin concentration

The tracings of attenuation coefficients during clot formation are shown in Fig. 3A, providing information on clot formation kinetics with different kaolin concentrations. Three distinct stages can be identified during blood coagulation. The changes of viscosity during blood coagulation were modeled approximately by a logistic function [29]. Figure 3B shows three stages in the sample with a kaolin concentration of 0.38 g/L. In the first stage, the blood is in a liquid state: the initial attenuation coefficient remains almost unchanged. During the second stage, fibrinogen begins to transform into fibrin through coagulation cascade reaction while the blood starts to clot. The attenuation coefficient increases markedly with progressively increasing viscosity. In the final stage, the attenuation coefficient changes to a small extent with an approximate horizontal asymptote corresponding to the stable and maximum viscosity of the clot. The time of the first stage indicates the initial coagulation time and the slope of the second stage characterizes the clot formation rates. In Fig. 3C, the coagulation metrics, including the initial coagulation time and the clot formation rate, are compared in the samples with different kaolin concentrations. The initial coagulation time is significantly increased in the samples with a lower kaolin concentration ($P<0.01$); however, the clot formation rates are similar in two groups of samples ($P>0.05$), which correspond with previous studies [16].

C. Blood coagulation with different diluted solutions

The tracings of attenuation coefficients in whole blood samples either diluted with NaCl or HES are shown in Fig. 4A. Similar to those in whole blood, the tracings in the samples diluted with NaCl can be separated into three distinct stages: a stable liquid state with low viscosity, a rapid transforming state and a stable gel state with high viscosity. The data from whole blood and blood diluted with NaCl were fitted into S-curves. However, in the samples diluted with HES, five distinct stages were observed, including a stable liquid state, first rapid transforming state, temporary stable state, second transforming state, and stable gel state. The data from blood diluted with HES were fitted into double S-curves. The data from the first rapid transforming state to the second transforming state were used to calculate the clot formation rates in the samples diluted with HES. In Fig. 4B, the initial coagulation time and the clot formation rate are compared among the whole blood samples, the blood samples diluted by NaCl and the blood samples diluted by HES. The initial coagulation time is similar in three groups of samples, indicating that the viscosity of these samples starts to change at a similar time. Clot initiation is quite resistant to hemodilution effects. After the blood starts to turn into a gel state, the clot formation rate is not significantly affected by hemodilution with NaCl ($P>0.05$) when the whole blood and the samples diluted with NaCl are compared. However, coagulation tracing and clot formation rate are significantly changed when the whole blood samples are diluted with HES. Clot formation significantly slows down after hemodilution with HES ($P<0.01$).

D. Discussion

The approach described here represents a coagulation test by measuring the attenuation coefficient within a very small amount of blood (200 μL). The attenuation coefficient of the compressional wave measured in our study depends on the tissue viscosity with a given wave frequency. Viscosity has been verified to be able to reflect actual coagulation processes [30]. Like most laboratory tests for blood coagulation, our coagulation assessment is made based on *in vitro* measurements. Coagulation metrics may vary between *in vitro* and *in vivo* tests due to the changes in flow conditions and contributions of endothelial cells [6]. However, the quantitative metrics are sensitive to the change in the coagulation properties from our measurements when the same volume of the blood is tested. More importantly, our measurements conduced on whole blood samples closely resembles the coagulation process *in vivo*. The foundation of the approach is a PZT-OCE system capable of real-time monitoring of the attenuation coefficient and quantitative measurements of clinically relevant coagulation metrics which, thus, produces assessment of coagulation status.

In order to monitor the blood coagulation, some methods have been proposed based on different physical measurements. Laser speckle rheology was developed to assess blood coagulation status by measurements of Brownian motion related to the viscoelastic properties of the medium [29]. The increase of viscoelasticiy deduces displacements of scatterers and, thus, slows down the rate of speckle fluctuations during the formation of the blood clot. The Brownian motion may be affected significantly by changes in the sizes of scatterers associated with aggregation of red blood cells during blood coagulation [31]. The quartz crystal biosensor, as a mechanical sensor, can detect the viscous changes based on frequency shift measurement on the surface of a sample during blood coagulation [32]. The coated surface of the quartz sensor is difficult to clean effectively and, thus, is consumable [33]. The TEG/ROTEM systems generate output by transforming the changes in the viscoelastic strength of clotting blood to the changes in the rotation of a pin in a rotating cuvette for coagulation assessment. The rotation of the pin begins to be triggered after fibrin-platelet bonding has linked the cup and pin together. Thus, the output of TEG/ROTEM is directly related to the strength of the formed clot [6]. However, the large sizes of TEG and ROTEM limit their clinical adoption for point-of-care applications. The complexity of TEG and ROTEM also results in the difficulties in operation [33]. Our PZT-OCE system visualizes the blood clot development in real-time by measurements of attenuation coefficients directly related to the tissue viscosity. OCT incorporating Doppler phase shift measurements can sensitively measure the vibration velocity in depth and, thus, accurately quantify the viscosity-related attenuation coefficient in real-time. The operation is simple and robust after loading the sample, and system size can be compact. Recently, the development of low-cost, portable OCT systems further reduces the cost while maintains the desired system performances [34]. Therefore, PZT-OCE has the potential as point-of-care testing for coagulation monitoring.

Acoustic radiation force orthogonal excitation optical coherence elastography (ARFOE-OCE) has also been developed to monitor blood coagulation based on measurements of shear wave propagation [16]. The application of ultrasonic force with water as a coupling medium increased the inconvenience of the measurements, and shear wave velocity

calculation also increased the complexity of data analysis. In order to visualize the shear wave propagation, 1 mL of sample volume was required. Compared with ARFOE-OCE, PZT-OCE measurements simplify the system and data analysis, and only 200 μL of sample volume is used.

We analyzed hemodilution using PZT-OCE in order to mimic blood loss and clinical infusion therapy. The PZT-OCE system successfully differentiated the difference between NaCl 0.9% and HES 6% in the diluted blood coagulation process. Coagulopathy induced by hemodilution with both NaCl 0.9% and HES 6% was characterized by a slower clot formation rate, but HES had a much more pronounced effect which is in accordance with previous studies [2]. HES 130/0.4, as a pump prime and intraoperative fluid therapy, was reported to significantly slow down clot formation [2]. These reportsare in accord with our measurements using the PZT-OCE system. In our measurements, the clot formation rate significantly slows down when the whole blood samples are diluted with HES.

IV. Conclusion

In this study, we developed a PZT-OCE system for monitoring blood coagulation based on the measurement of attenuation coefficients which is related to tissue viscosity with a given PZT driving frequency. The PZT-OCE system could be used to rapidly and conveniently gain information about clot formation process in whole blood. Clinically relevant coagulation metrics, including the initial coagulation time and the clot formation rate, were quantified to characterize the influence of the activator kaolin and the influence of hemodilution with either NaCl or HES on blood coagulation. PZT-OCE has the potential to be developed as point-of-care testing for diagnosis of coagulation disorders and monitoring of therapies, e.g., to characterize the range of acute coagulopathies present in patients with traumatic injury, identify the presence and type of coagulopathy at an early stage and, in turn, reveal the most appropriate treatment options for these patients in emergency settings.

Acknowledgment

Please address all correspondence to Dr. Z. Chen and Dr. X. Xu. Dr. Z. Chen has a financial interest in OCT Medical Imaging Inc., which, however, did not support this work.

X. Xu was supported by the National Natural Science Foundation of China (81171378) and Z. Chen was supported by the National Institutes of Health (R01HL-125084, R01HL-127271, R01EY-026091, R01EY-021529 and P41EB-015890).

Biography

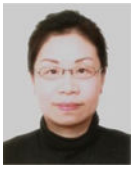

Xiangqun Xu received the B.Sc. degree in biochemistry from Xiamen University, Xiamen, China, in 1985, the M.Sc. degree in biochemistry from Zhejiang Medical University, Hangzhou, China, in 1997, and the Ph.D. degree in biomedical engineering from Keele

University, Keele, UK, in 2003. She is currently a professor in biomedical engineering at Zhejiang Sci-Tech University, Hangzhou, China. She received postdoctoral training in biomedical optics at Cranfield University, U.K. Her current research interests include optical coherence tomography and optical coherence elastography.

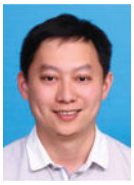

Jiang Zhu received the B.E. degree in Communication Engineering, and the M.E. degree in Microelectronics and Solid-State Electronics from Huazhong University of Science and Technology, Wuhan, China, in 2002 and 2004, respectively, and the Ph.D. degree in biology from Tsinghua University, Beijing, China, in 2009. He is currently a Postdoctoral Researcher at the Beckman Laser Institute, University of California, Irvine, Irvine, California, USA. His research interests include optical coherence tomography and optical coherence elastography.

Junxiao Yu received the B.E. degree in Biomedical Engineering from Illinois Institute of Technology, Chicago, IL, USA, in 2016. She is currently working toward the Ph.D. degree under the guidance of Dr. Z. Chen. Her research interests include optical coherence tomography and optical coherence elastography.

Zhongping Chen received the B.S. degree in applied physics from Shanghai Jiao Tong University, Shanghai, China, in 1982, and the M.S. degree in electrical engineering and the Ph.D. degree in applied physics both from Cornell University, Ithaca, NY, USA, in 1987 and 1993, respectively. He is currently a Professor of biomedical engineering and the Director of F-OCT Laboratory at the University of California, Irvine, CA, USA. He is a cofounder and the Board Chairman of OCT Medical Imaging, Inc. His research interests include the areas of biomedical photonics, microfabrication, biomaterials, and biosensors. His research group has pioneered the development of functional optical coherence tomography, which simultaneously provides high-resolution 3-D images of tissue structure, blood flow, and birefringence. He has published more than 220 peer-reviewed papers and review articles and holds a number of patents in the fields of biomaterials, biosensors, and biomedical imaging.

He is a Fellow of the American Institute of Medical and Biological Engineering, a Fellow of SPIE, and a Fellow of the Optical Society of America.

References

[1]. Kozek-Langenecker SA, “Fluids and coagulation,” Curr Opin Crit Care, vol. 21, no. 4, pp. 285–91, 8 2015. [PubMed: 26103143]

[2]. Hans GA, Hartstein G, Roediger L, Hubert B, Peters P, and Senard M, “Impact of 6 % hydroxyethyl starch (HES) 130/0.4 on the correlation between standard laboratory tests and thromboelastography (TEG®) after cardiopulmonary bypass,” Thromb Res, vol. 135, no. 5, pp. 984–9, 5 2015. [PubMed: 25769493]

[3]. Whiting D and DiNardo JA, “TEG and ROTEM: technology and clinical applications,” Am J Hematol, vol. 89, no. 2, pp. 228–32, 2 2014. [PubMed: 24123050]

[4]. Weber CF et al., “Point-of-care testing: a prospective, randomized clinical trial of efficacy in coagulopathic cardiac surgery patients,” Anesthesiology, vol. 117, no. 3, pp. 531–47, 9 2012. [PubMed: 22914710]

[5]. Schöchl H, Voelckel W, Grassetto A, and Schlimp CJ, “Practical application of point-of-care coagulation testing to guide treatment decisions in trauma,” J Trauma Acute Care Surg, vol. 74, no. 6, pp. 1587–98, 6 2013. [PubMed: 23694891]

[6]. Bolliger D, Seeberger MD, and Tanaka KA, “Principles and practice of thromboelastography in clinical coagulation management and transfusion practice,” Transfus Med Rev, vol. 26, no. 1, pp. 1–13, 1 2012. [PubMed: 21872428]

[7]. Kennedy B, Wijesinghe P, and Sampson D, “The emergence of optical elastography in biomedicine,” Nature Photonics, vol. 11, no. 4, pp. 215–221, 4 2017.

[8]. Larin KV and Sampson DD, “Optical coherence elastography - OCT at work in tissue biomechanics [Invited],” Biomed Opt Express, vol. 8, no. 2, pp. 1172–1202, 2 2017. [PubMed: 28271011]

[9]. Li Y, Jing J, Heidari E, Zhu J, Qu Y, and Chen Z, “Intravascular Optical Coherence Tomography for Characterization of Atherosclerosis with a 1.7 Micron Swept-Source Laser,” Sci Rep, vol. 7, no. 1, p. 14525, 11 2017. [PubMed: 29109462]

[10]. Chen Z and Zhu J, “Doppler optical coherence tomography and its application in measurement of cerebral blood flow,” in Neurophotonics and Brain Mapping, Chen Y and Kateb B, Eds. 1 ed Boca Raton: Taylor & Francis, 2017, pp. 159–176.

[11]. Chen Z and Zhang J, “Doppler Optical Coherence Tomography,” in Optical coherence tomography: technology and applications, Drexler W and Fujimoto JG, Eds. 2 ed Cham: Springer International Publishing, 2015, pp. 1289–1320.

[12]. Zhu J et al., “Longitudinal shear wave imaging for elasticity mapping using optical coherence elastography,” Appl Phys Lett, vol. 110, no. 20, p. 201101, 5 2017. [PubMed: 28611483]

[13]. Wang S et al., “Noncontact quantitative biomechanical characterization of cardiac muscle using shear wave imaging optical coherence tomography,” Biomed Opt Express, vol. 5, no. 7, pp. 1980–92, 7 2014. [PubMed: 25071943]

[14]. Zhu J et al., “Imaging and characterizing shear wave and shear modulus under orthogonal acoustic radiation force excitation using OCT Doppler variance method,” Opt Lett, vol. 40, no. 9, pp. 2099–102, 5 2015. [PubMed: 25927794]

[15]. Zhu J et al., “3D mapping of elastic modulus using shear wave optical micro-elastography,” Sci Rep, vol. 6, p. 35499, 10 2016. [PubMed: 27762276]

[16]. Xu X, Zhu J, and Chen Z, “Dynamic and quantitative assessment of blood coagulation using optical coherence elastography,” Sci Rep, vol. 6, p. 24294, 2016. [PubMed: 27090437]

[17]. Kennedy BF et al., “Optical coherence micro-elastography: mechanical-contrast imaging of tissue microstructure,” Biomed Opt Express, vol. 5, no. 7, pp. 2113–24, 7 2014. [PubMed: 25071952]

[18]. Nguyen TM, Song S, Arnal B, Huang Z, O’Donnell M, and Wang RK, “Visualizing ultrasonically induced shear wave propagation using phase-sensitive optical coherence

tomography for dynamic elastography," Opt Lett, vol. 39, no. 4, pp. 838–41, 2 2014. [PubMed: 24562220]

[19]. Qu Y et al., "Acoustic radiation force optical coherence elastography of corneal tissue," IEEE J Sel Topics Quantum Electron, vol. 22, no. 3, p. 6803507, May-Jun 2016.

[20]. Qu Y et al., "Miniature probe for mapping mechanical properties of vascular lesions using acoustic radiation force optical coherence elastography," Sci Rep, vol. 7, no. 1, p. 4731, 7 2017. [PubMed: 28680156]

[21]. Qu Y et al., "In Vivo Elasticity Mapping of Posterior Ocular Layers Using Acoustic Radiation Force Optical Coherence Elastography," Invest Ophthalmol Vis Sci, vol. 59, no. 1, pp. 455–461, 1 2018. [PubMed: 29368002]

[22]. Qi W et al., "Resonant acoustic radiation force optical coherence elastography," Appl Phys Lett, vol. 103, no. 10, p. 103704, 9 2013. [PubMed: 24086090]

[23]. Zhu J et al., "Quantitative angle-insensitive flow measurement using relative standard deviation OCT," Appl Phys Lett, vol. 111, no. 18, p. 181101, 10 2017. [PubMed: 29151604]

[24]. Meng J, Ding Z, Li J, Wang K, and Wu T, "Transit-time analysis based on delay-encoded beam shape for velocity vector quantification by spectral-domain Doppler optical coherence tomography," Opt Express, vol. 18, no. 2, pp. 1261–70, 1 2010. [PubMed: 20173950]

[25]. Zhao Y, Chen Z, Saxer C, Xiang S, de Boer JF, and Nelson JS, "Phase-resolved optical coherence tomography and optical Doppler tomography for imaging blood flow in human skin with fast scanning speed and high velocity sensitivity," Opt Lett, vol. 25, no. 2, pp. 114–6, 1 2000. [PubMed: 18059800]

[26]. Chen W and Holm S, "Modified Szabo's wave equation models for lossy media obeying frequency power law," J Acoust Soc Am, vol. 114, no. 5, pp. 2570–4, 11 2003. [PubMed: 14649993]

[27]. Shung KK, Diagnostic ultrasound: Imaging and blood flow measurements. Boca Raton, FL: Taylor & Francis, 2006.

[28]. Treeby BE, Zhang EZ, Thomas AS, and Cox BT, "Measurement of the ultrasound attenuation and dispersion in whole human blood and its components from 0–70 MHz," Ultrasound Med Biol, vol. 37, no. 2, pp. 289–300, 2 2011. [PubMed: 21208728]

[29]. Tripathi MM, Hajjarian Z, Van Cott EM, and Nadkarni SK, "Assessing blood coagulation status with laser speckle rheology," Biomed Opt Express, vol. 5, no. 3, pp. 817–31, 3 2014. [PubMed: 24688816]

[30]. Ranucci M, Laddomada T, and Baryshnikova E, "Blood viscosity during coagulation at different shear rates," Physiol Rep, vol. 2, no. 7, p. e12065, 7 2014. [PubMed: 24994896]

[31]. Huang CC, Wang SH, and Tsui PH, "Detection of blood coagulation and clot formation using quantitative ultrasonic parameters," Ultrasound Med Biol, vol. 31, no. 11, pp. 1567–73, 11 2005. [PubMed: 16286034]

[32]. Müller L et al., "Investigation of prothrombin time in human whole-blood samples with a quartz crystal biosensor," Anal Chem, vol. 82, no. 2, pp. 658–63, 1 2010. [PubMed: 20000697]

[33]. Harris L, Castro-Lopez V, and Killard A, "Coagulation monitoring devices: Past, present, and future at the point of care," TrAC Trends Anal Chem, vol. 50, pp. 85–95, 10 2013.

[34]. Kim S, Crose M, Eldridge WJ, Cox B, Brown WJ, and Wax A, "Design and implementation of a low-cost, portable OCT system," Biomed Opt Express, vol. 9, no. 3, pp. 1232–1243, 3 2018. [PubMed: 29541516]

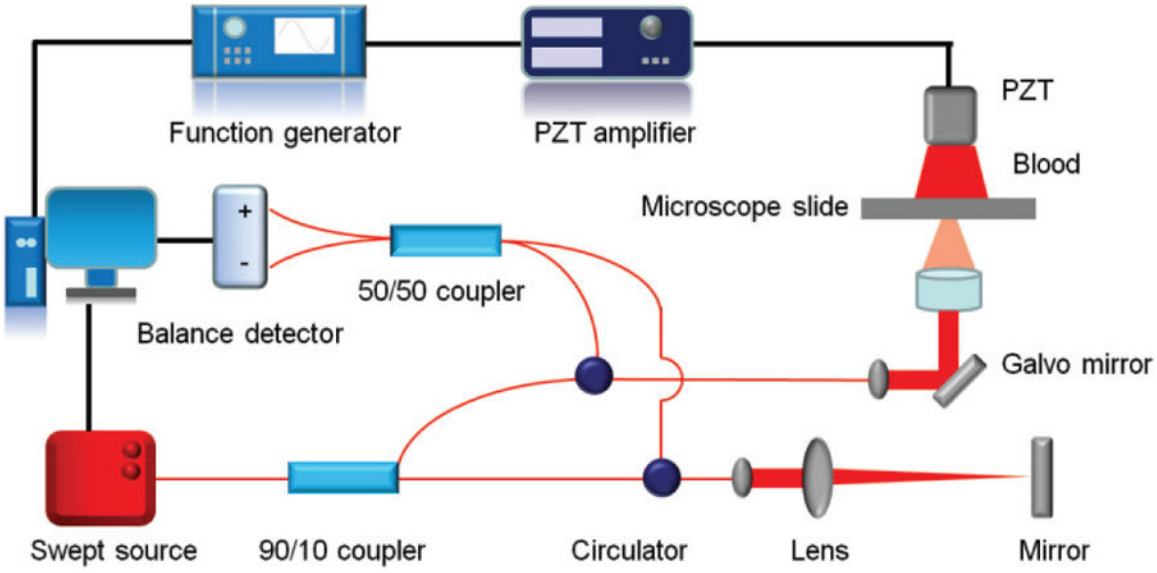

Fig. 1.

PZT-OCE system for blood coagulation monitoring. The PZT-induced vibration parallel to the OCT beam is detected by Doppler phase shift measurements.

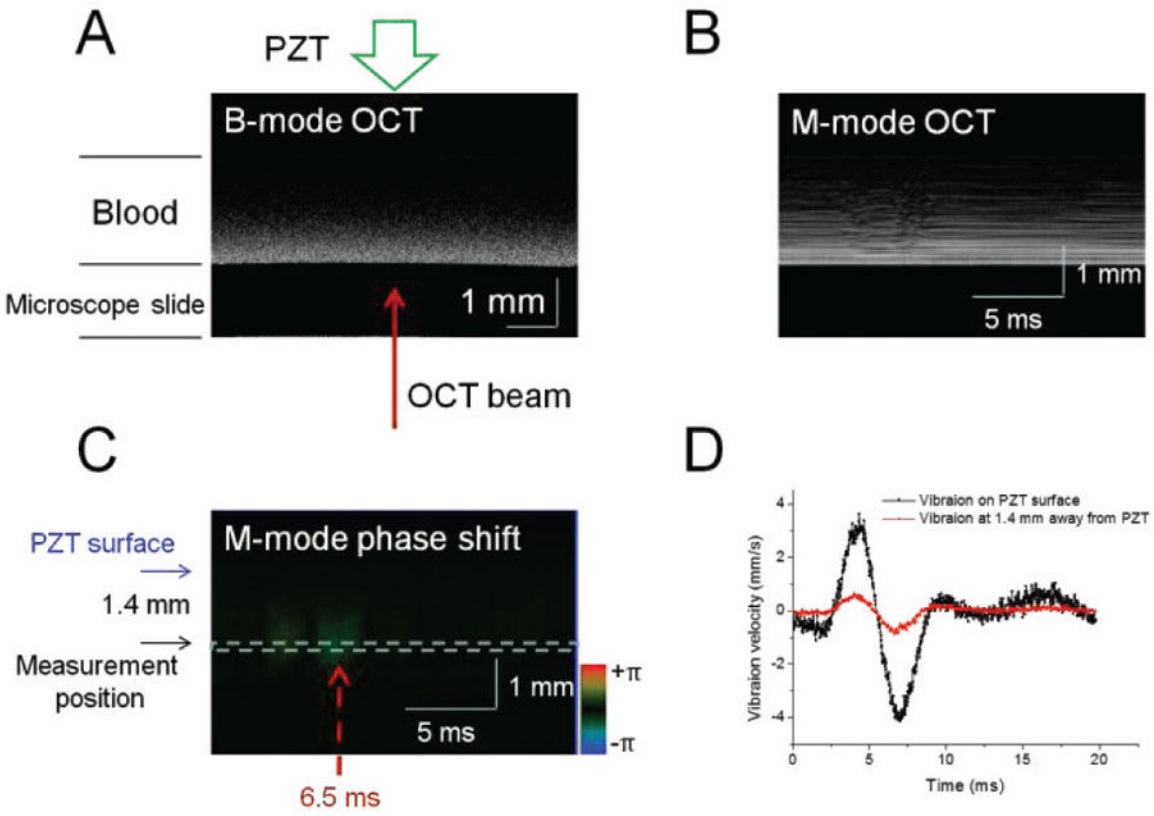

Fig. 2.

Vibration measurements in the blood sample. (A) OCT image in B-mode at 1 min after kaolin addition with a final concentration of 0.75 g/L. One M-scan OCT image (B) and the corresponding Doppler phase image (C) captured at 1 min following recalcification. The time interval Δt is 0.10 ms. (D) Vibration velocities on the PZT surface and 1.4 mm away from the PZT surface.

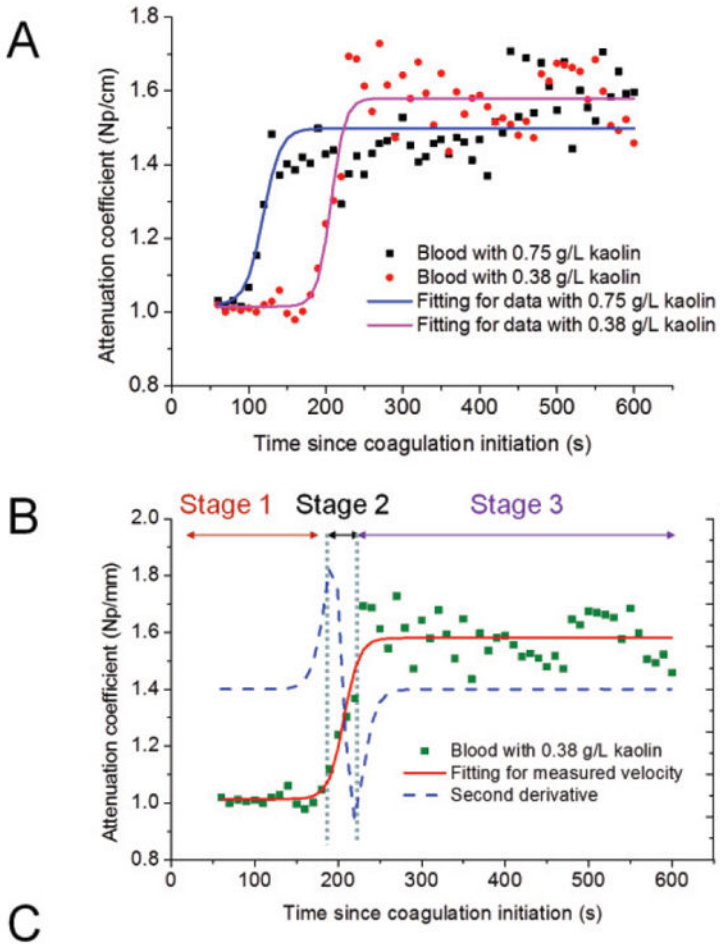

C

	Blood with 0.75 g/L kaolin	Blood with 0.38 g/L kaolin
Initial coagulation time [s]	103±6	193±6
Clot formation rate [Np/(mm·s)]	0.0113±0.0019	0.0133±0.0015

Fig. 3.

Monitoring of attenuation coefficients during blood coagulation in samples with different concentrations of kaolin solution. (A) Tracings of attenuation coefficients: three distinct stages are fitted into an S-curve. (B) Change of attenuation coefficients divided into three stages in the sample with a kaolin concentration of 0.38 g/L. (c) Coagulation metrics including the initial coagulation time and the clot formation rate: three samples for each group were tested.

A

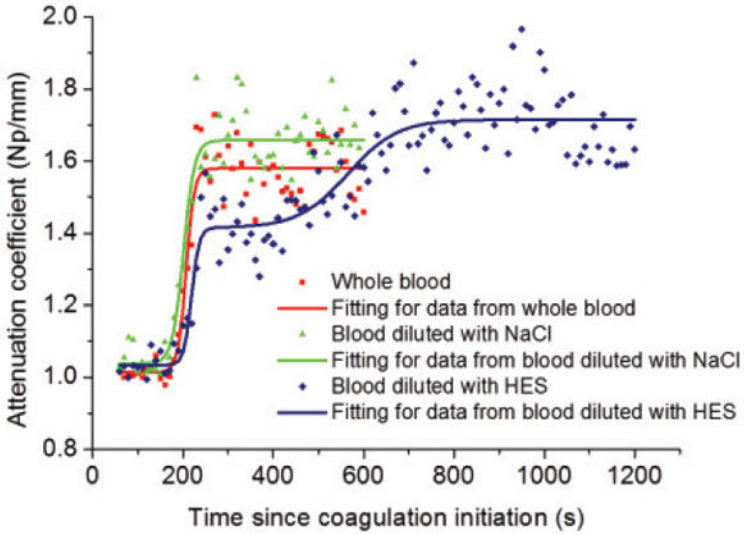

B

	Whole blood	Diluted with NaCl	Diluted with HES
Initial coagulation time [s]	193±6	183±15	200±10
Clot formation rate [Np/(mm·s)]	0.0133±0.0015	0.0110±0.0013	0.0015±0.0003

Fig. 4.

Monitoring of attenuation coefficients during blood coagulation in whole blood samples, samples diluted with NaCl and samples diluted with HES after kaolin addition with a concentration of 0.38 g/L. (A) Tracings of attenuation coefficients: the data from whole blood and NaCl diluted blood are fitted into S-curves, and the data from HES diluted blood are fitted into a double S-curve. (B) Initial coagulation time and clot formation rate in three groups of samples: three samples for each group were tested.